Heterogeneous Reactions of $HNO_3(g) + NaCl(s) \rightarrow HCl(g) + NaNO_3(s)$ and $N_2O_5(g) + NaCl(s) \rightarrow ClNO_2(g) + NaNO_3(s)$

Ming-Taun Leu,* Raimo S. Timonen, and Leon F. Keyser

Earth and Space Sciences Division, Jet Propulsion Laboratory, California Institute of Technology, Pasadena, California 91109

Yuk L. Yung

Division of Geological and Planetary Sciences, California Institute of Technology, Pasadena, California 91125

Received: February 9, 1995; In Final Form: June 29, 1995[⊗]

The heterogeneous reactions of $HNO_3(g) + NaCl(s) \rightarrow HCl(g) + NaNO_3(s)$ (eq 1) and $N_2O_5(g) + NaCl(s) \rightarrow ClNO_2(g) + NaNO_3(s)$ (eq 2) were investigated over the temperature range 223−296 K in a flow-tube reactor coupled to a quadrupole mass spectrometer. Either a chemical ionization mass spectrometer (CIMS) or an electron-impact ionization mass spectrometer (EIMS) was used to provide suitable detection sensitivity and selectivity. In order to mimic atmospheric conditions, partial pressures of HNO_3 and N_2O_5 in the range $6 \times 10^{-8} \sim 2 \times 10^{-6}$ Torr were used. Granule sizes and surface roughness of the solid NaCl substrates were determined by using a scanning electron microscope. For dry NaCl substrates, decay rates of HNO_3 were used to obtain $\gamma(1) = 0.013 \pm 0.004$ (1σ) at 296 K and >0.008 at 223 K, respectively. The error quoted is the statistical error. After all corrections were made, the overall error, including systematic error, was estimated to be about a factor of 2. HCl was found to be the sole gas-phase product of reaction 1. The mechanism changed from heterogeneous reaction to predominantly physical adsorption when the reactor was cooled from 296 to 223 K. For reaction 2 using dry salts, $\gamma(2)$ was found to be less than 1.0×10^{-4} at both 223 and 296 K. The gas-phase reaction product was identified as $ClNO_2$ in previous studies using an infrared spectrometer. An enhancement in reaction probability was observed if water was not completely removed from salt surfaces, probably due to the reaction of $N_2O_5(g) + H_2O(s) \rightarrow 2HNO_3(g)$. Our results are compared with previous literature values obtained using different experimental techniques and conditions. The implications of the present results for the enhancement of the hydrogen chloride column density in the lower stratosphere after the El Chichon volcanic eruption and for the chemistry of HCl and HNO_3 in the marine troposphere are discussed.

Introduction

The heterogeneous reactions of solid sodium chloride with atmospheric trace gases, for example HNO_3, N_2O_5, $ClONO_2$, and NO_2,

$$HNO_3(g) + NaCl(s) \rightarrow HCl(g) + NaNO_3(s), \quad \Delta H_0^{298K} = -3.3 \text{ kcal/mol} \quad (1)$$

$$N_2O_5(g) + NaCl(s) \rightarrow ClNO_2(g) + NaNO_3(s), \quad \Delta H_0^{298K} = -13.2 \text{ kcal/mol} \quad (2)$$

$$ClONO_2(g) + NaCl(s) \rightarrow Cl_2(g) + NaNO_3(s), \quad \Delta H_0^{298K} = -19.8 \text{ kcal/mol} \quad (3)$$

$$2NO_2(g) + NaCl(s) \rightarrow NOCl(g) + NaNO_3(s), \quad \Delta H_0^{298K} = -41.7 \text{ kcal/mol} \quad (4)$$

are of fundamental importance in atmospheric chemistry for the following reasons. First, it has been suggested that these reactions are responsible for the observed enhancement of the hydrogen chloride column density in the lower stratosphere after the El Chichon volcanic eruption. Second, reaction 1 can directly transform nitric acid into hydrogen chloride, which has been observed in the marine troposphere, resulting in a deficit of chloride in marine aerosols. Third, reactions 2−4 may be a potential source of reactive chlorine by converting solid sodium chloride into gaseous $ClNO_2$, Cl_2, and NOCl, which undergo photodissociation processes to produce atomic chlorine. These chlorine atoms then react with methane or other molecules, producing HCl. It is now well established that an enhancement of the chlorine budget can influence the catalytic destruction of stratospheric ozone.[1] Therefore, it is important to investigate these reactions not only by measuring their reaction probabilities but also by identifying their reaction mechanisms, using experimental conditions as close as possible to the ambient environment.

Salt particles were collected by a crystal-balanced cascade impactor from the El Chichon volcanic clouds in the lower stratosphere in the spring of 1982.[2] The number density was as much as 26 particles/cm^3 and the size was about 1−2 μm. Simultaneous measurements of the hydrogen chloride column density by a Fourier transform infrared spectrometer showed approximately a 40% enhancement over the background observed prior to the volcanic eruptions.[3] The observations of Mankin and Coffey[3] have recently been confirmed using the decadal record of HCl measurements taken at Jungfraujoch (Switzerland) by R. Zander (private communication, 1994). The heterogeneous reactions 1−4 have been suggested to play an important role in these observations.[4,5]

In the marine boundary layer, sea salt aerosols are generated

* Author to whom correspondence should be addressed.

[⊗] Abstract published in *Advance ACS Abstracts*, August 1, 1995.

0022-3654/95/2099-13203$09.00/0

by breaking waves on the ocean's surface. It has been observed that Na^+ is often in excess of Cl^- in aerosol samples, suggesting that sea salt reacts with NO_2, N_2O_5, HNO_3, or sulfate aerosols.[6-9] These reactions displace the chloride in aerosols and form HCl. In addition, reactions 2−4 may provide a source of atomic chlorine which removes alkanes and dimethyl sulfide (DMS). This reaction mechanism has also been suggested to explain numerous atmospheric observations of gaseous nitric acid, hydrochloric acid, and nitrate particulates in the eastern U.S.,[10] the greater Los Angeles area,[11,12] and the Hawaiian islands.[13]

There are several laboratory investigations of reactions 1−4. The reaction probability for reaction 1 has been reported in a recent preliminary study[14] using X-ray photoelectron spectroscopy to detect nitrate formation on single NaCl crystals in an ultrahigh vacuum chamber. This is a rather novel technique for surface reaction study, however, neither gaseous reactant nor gas-phase product was monitored in this study. Using a low-pressure flow reactor interfaced with a mass spectrometer, Fenter et al.[15] determined γ for reaction 1 at 298 K. HCl was found to be the sole gas-phase product of the reaction. Internal surface areas were not considered in the determination of $\gamma(1)$. It is somewhat surprising that these workers also obtained the same γ value for the uptake of HNO_3 on $NaNO_3$ substrates.

Using an infrared spectrometer, Livingston and Finlayson-Pitts[16] determined a lower limit for $\gamma(2)$. The initial concentration of N_2O_5 used in the reactor was 1.2×10^{14} molecules cm^{-3}, several orders of magnitude greater than the ambient concentration in the troposphere. The ratio $[HNO_3]/[N_2O_5] = 0.55$ in the N_2O_5/air mixtures was also measured. The reaction products were identified as $ClNO_2$ and HCl on the basis of their unique infrared spectra. The presence of the HNO_3 impurity may interfere with their study as discussed below. In a series of studies, Zetzsch and his co-workers[17-20] investigated the uptake of N_2O_5 by NaCl solutions from 262 to 278 K by using a droplet train technique, a wetted-wall column apparatus, and an aerosol chamber. The experimental conditions used are more relevant to tropospheric conditions, and the result is suitable for use in tropospheric modeling. Using a deposition profile measurement in an annular reactor and ion chromatography for nitrate analysis, Msibi et al.[21] obtained reaction probabilities for reaction 2 in both dry and wet NaCl substrates. The study requires a rather complicated procedure for the determination of γ.

For reaction 3, a summary of our work[22] using a fast flow-tube reactor interfaced to a quadrupole mass spectrometer has been recently published. Both the reactant decay and the product growth were used to determine the true reaction probability under stratospheric conditions. Reaction 4 has been shown to be too slow to be of importance in the atmosphere.[23]

In this article, we report the measurement of reaction probabilities for reactions 1 and 2 using partial pressures of reactants about 6×10^{-8} to 2×10^{-6} Torr encountered in the lower stratosphere and also in the marine boundary layer. First, we will describe the experimental procedures used, including the details of the recently developed chemical ionization mass spectrometer. Next, we will summarize and discuss the results of the reaction probability measurements and a kinetic mechanism for reaction 1. Finally, we will compare our data with previous measurements and discuss briefly the atmospheric implications of our present results.

Experimental Section

The reaction probability measurement was performed in a fast flow-tube reactor coupled to a quadrupole mass spectrometer. Two detection systems, a chemical ionization mass spectrometer (CIMS) and an electron-impact ionization mass

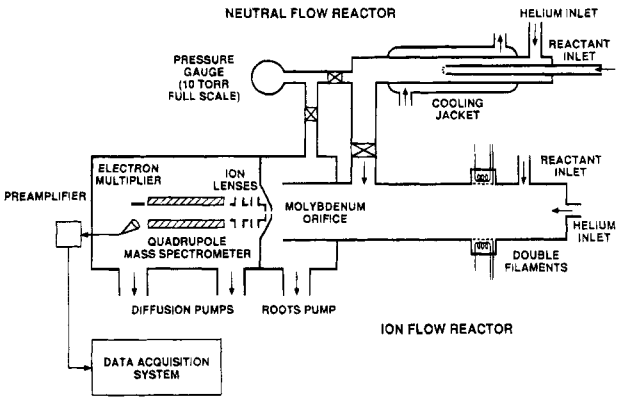

Figure 1. Schematic diagram of the neutral flow-tube reactor coupled to a chemical ionization mass spectrometer (CIMS). The bottom of the reactor was recessed and made flat in order to hold the NaCl substrates in place. See Figure 2 for details.

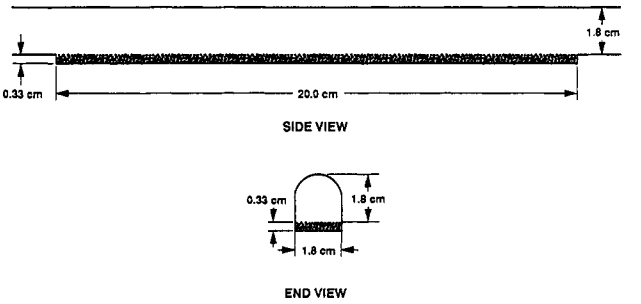

Figure 2. End view and side view of the flow-tube reactor. See text for details.

spectrometer (EIMS), were used depending upon the requirements of sensitivity and selectivity. The EIMS apparatus has been discussed in detail previously,[24,25] and the description will not be repeated in this article. However, the CIMS apparatus has been recently developed in this laboratory and will be described as follows.

Flow Reactor/Chemical Ionization Mass Spectrometer. The neutral flow reactor was made of borosilicate glass, and its dimensions are 20.0 cm in length and 1.8 cm i.d. (see Figures 1 and 2). The bottom of the reactor was recessed and made flat in order to hold the NaCl substrates in place. The depth of the recess is about 0.33 cm. The regulation of temperature was made possible by circulating cold methanol through the jacket surrounding the flow reactor, and the temperature was measured by a thermocouple attached to the middle section. The pressure inside the reactor was monitored by a high-precision capacitance manometer which was located about 7 cm from the reactor at the downstream end. The measured pressure was corrected for the viscous pressure gradient between the measurement point and the midpoint of the reactor. The carrier gas was helium and was admitted to the reactor through a side-arm inlet. The reactants, HNO_3 and N_2O_5, were added through a sliding borosilicate injector as shown in Figure 1. The average flow velocity in the neutral flow reactor was between 170 and 2800 cm/s. A large glass valve located at the downstream end of the neutral reactor was used to regulate the flow velocity.

A schematic diagram of the CIMS apparatus is shown in Figure 1. The design is similar to that used previously.[26] The ion flow reactor was constructed of a stainless steel tube of 127 cm in length and 7.0 cm i.d. A large flow of helium, 6−10 slpm (standard liter per minute at 293 K), was passed through the reactor at a constant pressure in the range 0.2−0.5 Torr. A large-capacity booster pump (Edwards High Vacuum, Model EH2600, 610 L/s) was used to evacuate the ion flow reactor. The average flow velocity used in the ion flow reactor was

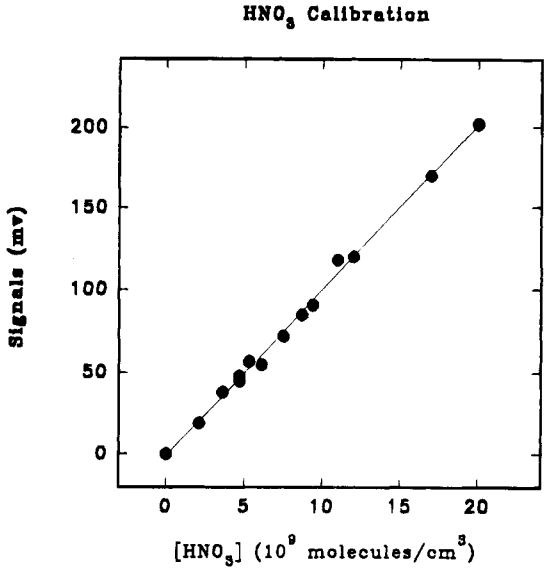

Figure 3. Calibration of HNO_3 signals as a function of concentration. The total pressure is 0.349 Torr, and the temperature is 296 K.

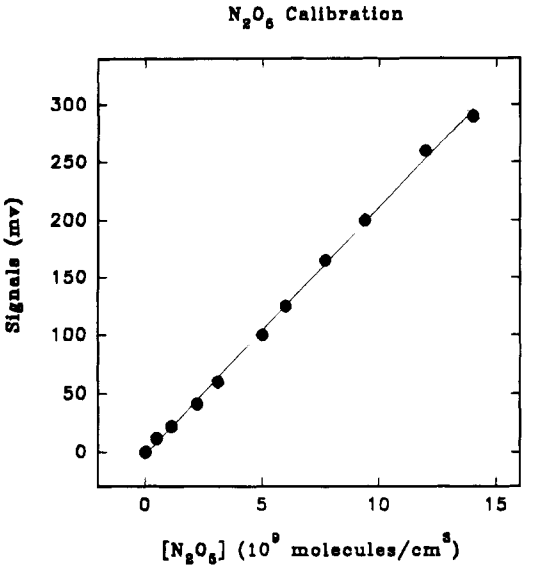

Figure 4. Calibration of N_2O_5 signals as a function of concentration. The total pressure is 0.431 Torr, and the temperature is 296 K.

typically about 100−160 m/s in these experiments. A small flow of SF_6, 1−5 sccm (standard cubic centimeter per minute at 293 K), was mixed with the helium carrier, and SF_6^- ions were formed by electron attachment. The electrons were produced by passing a current (6−10 A) through a filament located at a side-arm port of the reactor. The filament material was tungsten, rhenium, or thoriated iridium. SF_6^- ions were allowed to react with the trace gas species from the neutral flow reactor, for example, HNO_3 by the reaction

$$SF_6^- + HNO_3 \rightarrow NO_3^-(HF) + SF_5 \quad (k = 1.8 \times 10^{-9}\ cm^3/s^{27,28}) \quad (5)$$

These ions were then effused through a molybdenum orifice (0.5 mm in diameter) and collimated by a set of ion lenses. The first lens was separated from the molybdenum orifice about 0.5 cm and was biased by a small voltage (1−10 V) in order to focus the ions through the lens system. A quadrupole mass spectrometer (a set of quadrupole rods 9 in. in length and $^5/_8$ in. o.d. powered by a C-60 electronics module) was used to analyze these ions (for example, 146 amu for SF_6^- and 82 amu for $NO_3^-(HF)$). The ion signals were amplified by a conversion dynode/electron multiplier and then recorded by an electrometer (Extrel Corp., Model 031-2). A minicomputer was used to acquire the data for further analysis. The calibration of HNO_3 signals is shown in Figure 3. The experimental procedure is accomplished by preparing a known amount of HNO_3 vapor in a helium carrier in a glass vessel and measuring its flow rate. The dynamic range is linear up to 3×10^{11} molecules/cm^3 (or 1×10^{-5} Torr). The detection sensitivity for HNO_3 using this technique is about 2×10^8 molecules/cm^3 (or 6×10^{-9} Torr and S/N = 1 for 1 s integration). The detection sensitivity is more than adequate for the present experiment. Further improvement is possible by using a new electron multiplier.

The detection of N_2O_5 in the presence of HNO_3 was performed in the same manner. The reagent ions I^- were generated from the dissociative attachment of CF_3I by electrons. The detection of I^- was made by using the reaction

$$I^- + N_2O_5 \rightarrow NO_3^- + INO_2 \quad (k = 1.3 \times 10^{-9}\ cm^3/s^{27,29}) \quad (6)$$

The rate coefficient for reaction 6 is several orders of magnitude greater than that for the $I^- + HNO_3 \rightarrow NO_3^- + HI$ reaction (<1.0×10^{-12} cm^3/s).[27] Thus, it is possible to detect N_2O_5 selectively in the presence of HNO_3. The calibration of N_2O_5 signals is similar to that of HNO_3 signals and is shown in Figure 4. The dynamic range is also linear up to 3×10^{11} molecules/cm^3 (or 1×10^{-5} Torr). Currently, the detection limit for N_2O_5 is about 1×10^8 molecules/cm^3 (or about 3×10^{-9} Torr and S/N = 1 for 1 s integration) using this CIMS apparatus. Again, the selective detection of N_2O_5 is adequate for this experiment.

Synthesis of HNO_3 and N_2O_5. HNO_3 was prepared by reacting H_2SO_4 (96 wt % purity liquid) with reagent grade $NaNO_3$ (99 % purity solid) in vacuum, and the nitric acid vapor was collected in a Pyrex vessel at liquid nitrogen temperature. The HNO_3 thus prepared was further purified by vacuum distillation at 195 K. N_2O_5 was prepared by mixing NO_2 with an excess of O_3 from an ozonizer. The N_2O_5 was stored at 195 K before use. The HNO_3 impurity in N_2O_5 inside the flow-tube reactor was checked with a CIMS and was found to be less than 10%. The interference of this impurity in the detection of N_2O_5 is negligible, as discussed in the previous paragraph.

The calibration of HNO_3 concentrations inside the flow reactor was accomplished by preparing a known amount of HNO_3 vapor in helium carrier gas in a glass vessel and measuring its flow rates. A similar procedure was also used for N_2O_5.

Preparation of the NaCl Substrates. NaCl crystals (>99.8% purity, analytical reagent) were supplied by J. T. Baker, Inc. The impurity levels of bromine or iodine compounds, which may react with HNO_3 or N_2O_5, were stated to be less than 0.005% and 0.001%, respectively. The size and shape of these crystals were examined by using a scanning electron microscope, and the typical shape of the NaCl particles is cubic and the average size is about 0.44 mm. The BET specific surface area of these samples was found to be about 100 (+100, −50) cm^2/g. The specific surface area, S_g, was also calculated from the average crystal size by using the following equation[30]

$$S_g = 6/\varrho_t d \quad (7)$$

where ϱ_t is the true density of NaCl (2.165 g/cm^3)[31] and d is the particle size. Using d = 0.44 mm obtained from the SEM experiments, we obtain a surface area of 63 cm^2/g from eq 7, which is in agreement with the BET surface area within the stated experimental error.

The NaCl substrates were prepared in such a way to simulate the aerosol conditions encountered in the stratosphere after a volcanic eruption. In one set of the experiments the granules were baked at temperatures up to 473 K in the flow reactor overnight; the H_2O vapor pressure over these substrates was measured to be less than 2×10^{-5} Torr using the EIMS apparatus. In another set of the experiments, the granules were held in a flow reactor and a stream of H_2O vapor was passed over the NaCl granules; the H_2O vapor pressure was kept in the range 2×10^{-5} to 2×10^{-4} Torr. The temperature of the NaCl substrates inside the reactor was regulated between 223 and 296 K. The thickness of the NaCl substrates inside the reactor was varied from 1.0 to 4.0 mm. Thus, the number of granule layers for the NaCl substrates is about 2−9.

Some experiments were performed using solid sodium chloride crystals which were supplied from Solon Technologies, Inc. These crystals were polished and cleaved in the (100) plane. Their dimensions are 25 mm × 12 mm × 2 mm. They were spread over the bottom of the flow reactor. It is reasonable to assume that only the geometric area of these crystals is available for reaction with HNO_3.

Procedures for Reaction Probability Measurements. The reaction probabilities for reactions 1 and 2 were determined as follows. The loss rates of HNO_3 and N_2O_5 were measured as a function of inlet position, z. The reaction time was calculated by using $t = z/v$, where v is the average flow velocity. In each experiment we calculated the cross-sectional area of the reactor and then the flow velocity. The first-order rate constant, k_s, was calculated from the slope of a linear least-squares fit to the experimental data. The axial gas-phase diffusion correction for k_s was made by using the following equation[32,33]

$$k_g = k_s(1 + k_s D/v^2) \tag{8}$$

The diffusion coefficients of HNO_3 and N_2O_5 in helium were estimated to be pD = 495 and 350 Torr cm^2 s^{-1} at 296 K, respectively.[34] A temperature coefficient of $T^{1.76}$ for the diffusion coefficient was also assumed. The rate corrected for gas-phase diffusion is designated as k_g.

For radial gas-phase diffusion, it is more difficult to estimate the correction to k_s because the reactor is no longer a fully symmetric cylindrical tube. If we use the full reactor radius of 0.9 cm in the calculation, the correction is relatively small, less than 10%. Since this correction is not precise, we neglected it in the data analysis.

On the basis of the geometric area, S, of the NaCl substrate and the volume, V, of the reactor, the reaction probability, γ_g, was then calculated by using the following equation[35,36]

$$\gamma_g = 4k_g V/\bar{\omega} S \tag{9}$$

where $\bar{\omega}$ is the average molecular velocity for HNO_3 or N_2O_5. Note that this equation is valid for $\gamma_g < 0.1$ only, which holds for the present experiments.

To account for the surfaces of the salt granules beneath the top layer, we used an analysis recently developed and successfully applied to heterogeneous reactions on porous ice films.[35,36] We model the NaCl substrate as hexagonal close-packed (HCP) spherical granules stacked in layers. For this model, the following equation holds

$$\gamma_t = \gamma_g \pi^{-1} 3^{1/2}\{1 + \eta[2(N_L - 1) + (3/2)^{1/2}]\}^{-1} \tag{10}$$

where γ_t is the true reaction probability for reactions 1 and 2 and N_L is the number of granule layers or the ratio of the thickness of the NaCl substrates to the average granule size. In eq 10, η is the effectiveness factor, which is the fraction of the NaCl surface that participates in the reaction. This factor is determined by the relative rates of pore diffusion to surface reaction and is given by

$$\eta = \phi^{-1} \tanh \phi \tag{11}$$

$$\phi = (h/d)[3\varrho_b/2(\varrho_t - \varrho_b)](3\tau\gamma_t)^{1/2} \tag{12}$$

where h is the substrate thickness, d is the average size of granules, ϱ_b is the bulk density, ϱ_t is the true density, and τ is a tortuosity factor. Typically, this factor is between 1.7 and 4.[37] In our data analysis, we used a value of 2. This type of calculation has been used and discussed in previous publications.[22,24,25]

In general, the magnitude of the corrections that convert γ_g to γ_t is less than a factor of 3 for $\gamma_t > 0.1$. However, for $\gamma_t < 0.1$, the corrections become much larger.[35,36] The possible uncertainties in the correction factors can be estimated by assessing the expected errors introduced by uncertainties in N_L, τ, and the type of packing (bulk density). For an uncertainty in N_L of ±2 within the range used, the errors in the correction factors are less than 15%. For $\tau = 2$ or 3,[37] the error in the correction factors is less than ±20%. For layer packing between simple cubic packing (SCP) and HCP, the correction factor error ranges over ±25%. Including the errors (~15−25%) associated with the measurements of temperature, total pressure, flow rates, and external gas-phase diffusion correction, we estimate the systematic error is about a factor of 2.

Results

$HNO_3 + NaCl \rightarrow HCl + NaNO_3$ (1). The uptake of HNO_3 in the presence of baked NaCl substrate at 296 K is shown in Figure 5a. This experiment was performed using the EIMS apparatus, and both HNO_3 and HCl were monitored using 46 and 36 amu, respectively. The Pyrex injector was moved upstream and downstream of the flow-tube reactor in this series of experiments. The experimental conditions used were m(NaCl) = 5.0 g, p(total) = 0.308 Torr, v = 1051 cm/s, and $p(HNO_3) = 6.7 \times 10^{-7}$ Torr. The reaction product, HCl, was produced readily, and its yield was found to be near unity. To test the surface deactivation, another experiment was performed for a much longer reaction time (shown in Figure 5b). The experimental conditions were m(NaCl) = 5.0 g, p(total) = 0.343 Torr, v = 1276 cm/s, and $p(HNO_3) = 1.7 \times 10^{-6}$ Torr. It is intriguing to note that the NaCl surface is not completely saturated even after 3 h of exposure of HNO_3 and the amount of HNO_3 uptake ($>1.1 \times 10^{15}$ molecules/cm^2) is greater than one monolayer ($\sim 6 \times 10^{14}$ molecules/cm^2). It is possible that, during the reaction, the NaCl surface may form microcrystallites of $NaNO_3$, regenerating fresh NaCl surfaces for further reaction.[23] In other words, the crystal lattice of NaCl may be ruptured during the reaction. Another possibility is the diffusion of nitric acid through the solid salts. This type of uptake behavior is consistent with our previous work on the uptake of $ClONO_2$ by NaCl substrates at 296 K.[22]

In order to provide data for stratospheric modeling, a similar experiment was also carried out at a temperature of 223 K and the result is shown in Figure 6a. The experimental conditions were m(NaCl) = 5.0 g, v = 1120 cm/s, p(total) = 0.321 Torr, and $p(HCl) = 1.8 \times 10^{-6}$ Torr. In addition to heterogeneous reaction 1 there was a marked physical adsorption of HNO_3 on the NaCl surface. Furthermore, the surface was deactivated rapidly within about 10 min, much shorter than that in the experiment at 296 K. By pushing the injector back to the

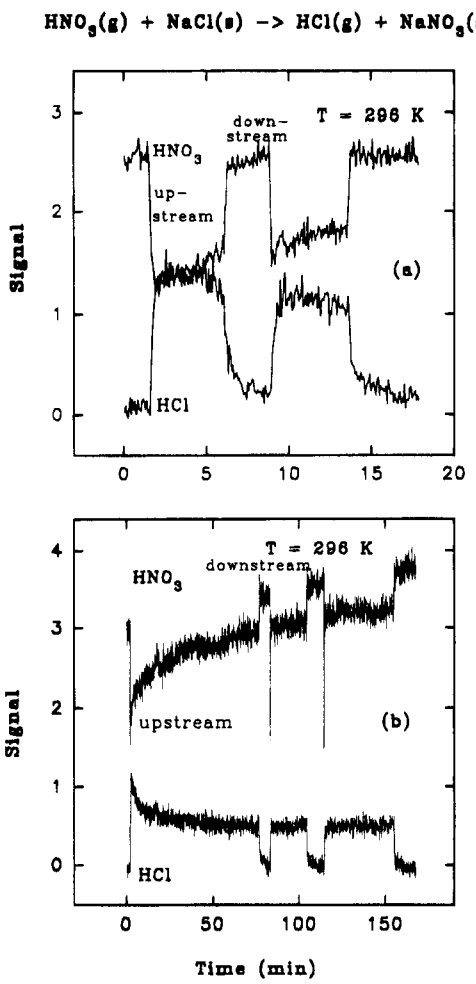

Figure 5. Uptake of HNO by NaCl at 296 K. Both the HNO_3 loss and HCl growth are monitored: (a) for reaction times up to 18 min and (b) for reaction times as long as 3 h.

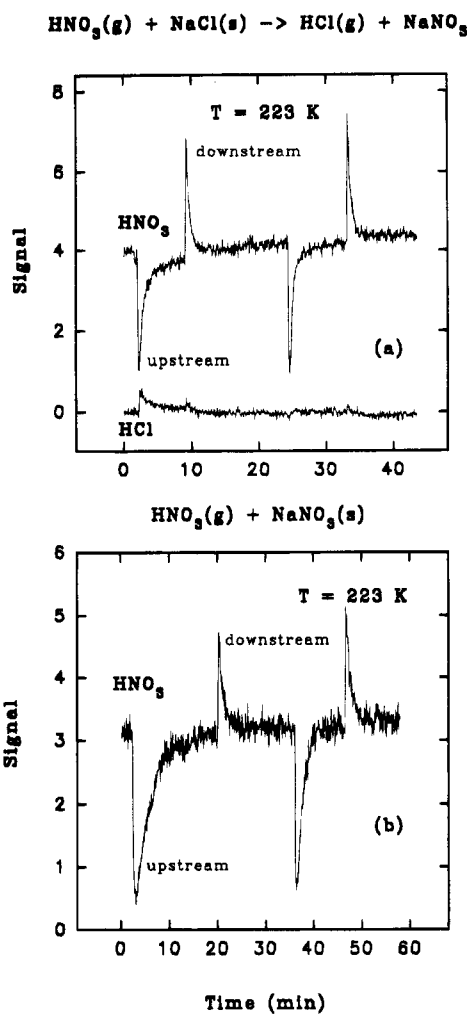

Figure 6. (a) Uptake of HNO_3 by NaCl at 223 K. Both physical adsorption and heterogeneous reaction are evident. (b) Physical uptake of HNO by $NaNO_3$ at 223 K.

original position and allowing the warm Pyrex injector to anneal the substrates, the amount of HNO_3 desorbed was about 90–95% of the HNO_3 uptake. Nonetheless, the HCl yield (about 5–10% of the HNO_3 uptake) is much smaller than that at 296 K. The rapid surface deactivation effect may interfere with the determination of the γ value which will be discussed later.

To test this hypothesis, we also performed an experiment on the physical uptake of HNO_3 on $NaNO_3$ solid. The result at 223 K is shown in Figure 6b. Similar kinetic behavior as shown in Figure 6a was observed. The desorption peak was always smaller than the adsorption peak, suggesting some of the HNO_3 may stay on the surface. Furthermore, no reaction product was found in this experiment. The results found at 296 and 253 K are similar to that shown in Figure 6b, suggesting a physical uptake of HNO_3 on $NaNO_3$ surfaces. We did not attempt to measure the effective γ value for this uptake process.

For an irreversible pseudo-first-order reaction under plug-flow conditions, the decay of HNO_3 is given by the equation[22,25]

$$\ln[S(z)] = -k_s(z/v) + \ln[S(0)] \qquad (13)$$

where $S(z)$ is the HNO_3 signal when the injector is at z, $S(0)$ is the signal when the NaCl is bypassed, and z/v is the reaction time. The observed rates, k_s, are determined from the slopes of linear least-squares fits to these data.

Typical data of the HNO_3 loss as a function of injector position at 295 K are shown in Figure 7. The CIMS apparatus was used for the detection of HNO_3 in this experiment. The experimental conditions were $m(NaCl) = 22$ g, $v = 2738$ cm/s,

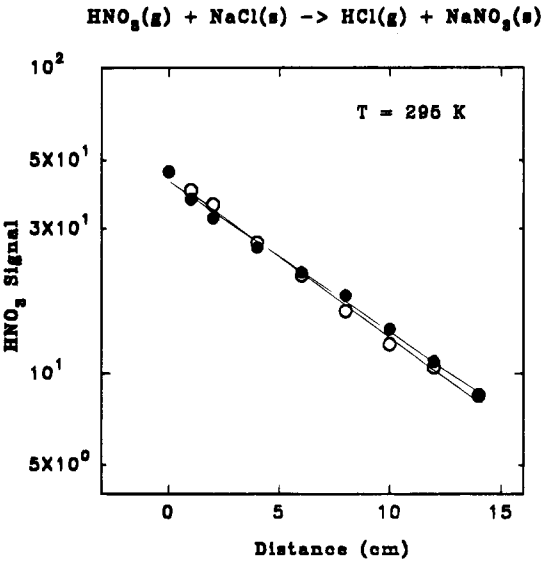

Figure 7. Loss of HNO_3 signals as a function of injector position at 295 K. Open circles are for data obtained from the injector moving from downstream to upstream. Closed circles are for data obtained from the injector moving from upstream to downstream. See text for details.

and $p(HNO_3) = 7.9 \times 10^{-8}$ Torr. The salts were baked overnight in vacuum before use. In the absence of the NaCl substrates, the HNO_3 signals are independent of the injector position, providing evidence that the physical adsorption of

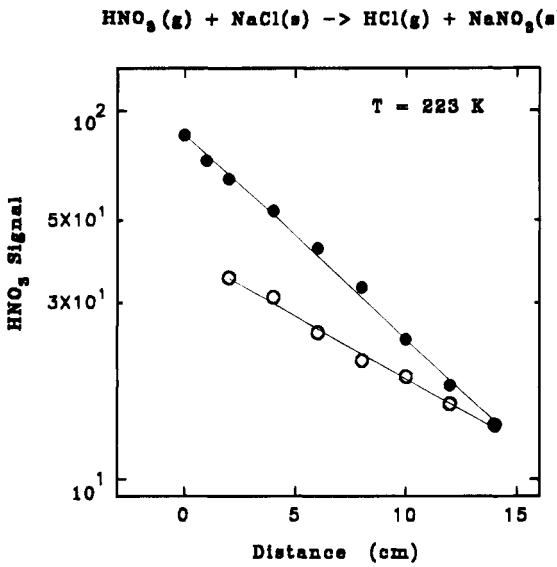

Figure 8. Loss of HNO_3 signals as a function of injector position at 223 K. Open circles are for data obtained from the injector moving from downstream to upstream. Closed circles are for data obtained from the injector moving from upstream to downstream. See text for details.

HNO_3 on the surfaces of the flow-tube reactor was negligible, consistent with the data shown in Figure 5. With NaCl present, the decay of the HNO_3 signals was linear according to eq 13, which suggests that the pseudo-first-order condition is valid. The rate determined as the injector was pulled-out (from downstream to upstream) is nearly identical to that when the injector was pushed-in (from upstream to downstream). Using the procedures discussed in a previous section, an average value of $\gamma(1) = 0.013$ was obtained.

A similar experiment was also performed at 223 K, and the result is shown in Figure 8. The experimental conditions used were $m(\text{NaCl}) = 20$ g, $v = 1728$ cm/s, and $p(HNO_3)$ 6.9×10^{-8} Torr. The NaCl substrates were baked overnight in vacuum. It is evident that the rate observed when the injector was moved from downstream to upstream is smaller than that observed when the injector was moved from upstream to downstream because of the adsorption/desorption processes of HNO_3 occurring on the NaCl surface. A value of $\gamma = 0.005$ was determined only from the data when the injector was moved from downstream to upstream, and this should represent a lower limit for reaction 1 at 223 K. A weak signal of HCl was also observed, possibly due to the adsorption of HCl on the NaCl surface.

The experimental conditions used in the determination of the reaction probabilities for reaction 1 are summarized in Table 1. Initial HNO_3 pressures were varied from 6.5×10^{-8} to 1.1×10^{-6} Torr, and the temperature was varied from 223 to 296 K in these experiments. The γ values are approximately independent of the NaCl preparation (baked, unbaked, or water vapor added). The average value is 0.013 ± 0.004 at 296 K and >0.008 at 223 K, respectively. The error quoted is one standard deviation. It is of interest to note that the uptake coefficients apparently depend on $p(HNO_3)$ used because of the surface deactivation. For example, the data collected at lower reactant pressures at room temperature are about a factor of 2 greater than those using larger reactant pressures as registered in Table 1. Several preliminary experiments were performed using much larger HNO_3 pressures about $(1-3) \times 10^{-5}$ Torr; γ values were found to be about 0.0004 at 296 K, much smaller than that listed in Table 1. Apparently, surface saturation plays an important role in these measurements.

A few experiments were performed by placing seven pieces of single crystals (25 mm × 12 mm × 2 mm, optical quality, supplied by Solon Technologies, Inc.) at the bottom of the flow reactor. The crystals were evacuated for a few hours at 296 K. We carried out the experiment in the same manner as that for the powder substrates using a partial pressure of HNO_3 about 2.5×10^{-6} Torr and obtained a value of $\gamma = (2.4 \pm 0.6) \times 10^{-3}$. To minimize the surface deactivation, we used a reaction time of 10−20 s, which is much shorter than we used in the powder experiments. However, because of the smaller surface area associated with single crystals, the deactivation is rather serious, and for this reason we believe that the lower γ value obtained in this experiment may be considered as a lower limit for reaction 1. Alternatively, the lower γ may be due to a smaller number of active sites per unit area available for reaction in single crystals.

$N_2O_5 + NaCl \rightarrow ClNO_2 + NaNO_3$ (2). The reaction probability for reaction 2 has been measured in a similar manner as that for reaction 1. Typical data are shown in Figure 9. The experimental conditions were $m(\text{NaCl}) = 20$ g, $p(\text{total}) = 1.346$ Torr, $v = 518$ cm/s, $T = 296$ K, and $p(N_2O_5) = 2.1 \times 10^{-6}$ Torr. The salts were not baked but evacuated in vacuum for a couple of hours. The N_2O_5 signals using the CIMS apparatus were monitored as a function of the sliding injector position in the presence and absence of the NaCl substrates. The uptake of N_2O_5 on the Pyrex surface is negligible. An average value of $\gamma(2) = 4.5 \times 10^{-4}$ was obtained on the basis of the loss rate of N_2O_5 signals. In other experiments for baked NaCl substrates, the decay rates, k_s, were always smaller than 10 s^{-1}. Using the procedures discussed in the previous section, $\gamma(2)$ was found to be less than 1×10^{-4} at both 223 and 296 K for dry NaCl substrates. For unbaked salts, $\gamma(2)$ is slightly enhanced, probably due to the reaction of $N_2O_5 + H_2O \rightarrow 2HNO_3$ on salt surfaces followed by reaction 1. These results are summarized in Table 2.

Discussion

In this article we report $\gamma(1) = 0.013 \pm 0.004$ at 296 K and >0.008 at 223 K, respectively, using a fast flow-reactor coupled to a quadrupole mass spectrometer. HCl is the sole gas-phase product of reaction 1. In addition, an upper limit of 1.0×10^{-4} for $\gamma(2)$ in the temperature range 223−296 K was also determined for dry NaCl granules. An enhancement in reactivity was also measured for slightly wet salts, apparently due to the reaction of $N_2O_5 + H_2O \rightarrow 2HNO_3$ on the NaCl surfaces. In Table 3 we compare our present results with literature values.

Comparison with Previous Measurements. Using X-ray photoelectron spectroscopy to follow the formation of nitrate on the surfaces of single crystals of NaCl, Laux et al.[14] obtained a value of $\gamma(1) = (4 \pm 2) \times 10^{-4}$ at 298 K, which is about a factor of 30 smaller than our data summarized in Table 1. Also, their value is much smaller than our lower limit data using single NaCl crystals. In their study no gas-phase products were reported. The NaCl crystals were placed in an ultrahigh vacuum chamber; thus, the surface should be free of significant amounts of water. Since the surface areas of the NaCl crystals were very smooth (single crystals were used), significant surface saturation took place in their experiments, as shown in Figure 3 of ref 14. Therefore, the observed γ value should be considered as a lower limit.

Rossi and his co-workers[15] investigated the uptake of nitric acid by solid salts and obtained a value of $\gamma(1) = (2.8 \pm 0.3) \times 10^{-2}$ at room temperature using a low-pressure flow reactor interfaced with a mass spectrometer. A similar value was also determined for the uptake of HNO_3 by the $NaNO_3$ powder, and this result is surprising because these uptake mechanisms are

TABLE 1: Summary of the Reaction Probability Measurements for the HNO_3 + NaCl → HCl + $NaNO_3$ Reaction with a Total Pressure about 0.45 Torr in All Experiments

$p(HNO_3)$, Torr	m(NaCl), g	T, K	v, cm/s	k_s, 1/s	k_g, 1/s	γ_g	γ_t	$p(H_2O)$, Torr	notes
7.9(−8)	22	295	2738	322	337	0.069	0.015	<2(−5)	*a*
1.1(−7)	22	293	2756	337	353	0.072	0.016	1.8(−4)	*c*
1.1(−7)	22	294	2699	303	317	0.065	0.014	<2(−5)	*a*
1.2(−7)	22	295	2828	380	400	0.082	0.019	2.1(−4)	*c*
1.2(−7)	22	294	2721	347	365	0.074	0.016	1.5(−4)	*c*
1.4(−7)	22	295	2767	380	401	0.082	0.019	8.1(−5)	*c*
2.6(−7)	20	292	2445	289	304	0.062	0.013	<2(−5)	*a*
2.9(−7)	18	296	2346	276	291	0.059	0.012	<2(−5)	*a*
3.1(−7)	20	295	2342	306	321	0.065	0.014	<2(−5)	*b*
3.4(−7)	20	295	1977	263	282	0.056	0.011	<2(−5)	*a*
4.0(−7)	18	294	2345	256	269	0.055	0.011	<2(−5)	*a*
6.0(−7)	20	297	2188	194	204	0.042	0.007	<2(−5)	*a*
6.4(−7)	20	294	1844	220	231	0.047	0.008	<2(−5)	*a*
1.1(−6)	20	294	2124	178	187	0.038	0.006	<2(−5)	*b*
						average value = 0.013 ± 0.004			
6.5 (−8)	20	223	2114	182	187	0.044	0.008	<2(−5)	*a*
6.9(−8)	20	223	1728	134	138	0.032	0.005	<2(−5)	*a*
7.1(−8)	20	223	2282	189	195	0.046	0.008	<2(−5)	*a*
7.1(−8)	22	223	2311	229	236	0.055	0.011	1.5(−4)	*c*
7.3(−8)	20	223	2342	193	199	0.047	0.008	<2(−5)	*a*
8.3(−8)	22	223	2229	283	291	0.068	0.015	<2(−5)	*a*
9.2(−8)	22	223	2252	208	214	0.050	0.009	<2(−5)	*a*
9.7(−8)	20	223	1797	192	198	0.047	0.008	1.2(−4)	*c*
9.7(−8)	22	223	2312	211	217	0.051	0.010	1.1(−4)	*c*
1.0(−7)	20	223	2169	181	186	0.044	0.008	9.5(−5)	*c*
1.2(−7)	20	223	2171	211	217	0.051	0.008	<2(−5)	*b*
1.2(−7)	20	223	2191	239	246	0.058	0.012	1.6(−4)	*c*
1.3(−7)	20	223	2113	206	212	0.050	0.009	<2(−5)	*a*
1.3(−7)	20	223	1757	109	112	0.026	0.003	<2(−5)	*a*
1.4(−7)	20	223	2220	213	219	0.051	0.008	1.8(−4)	*c*
1.4(−7)	20	223	2104	115	118	0.028	0.004	1.4(−4)	*c*
						average value = 0.008 ± 0.003			*d*

[a] NaCl substrates were baked overnight in vacuum. [b] NaCl substrates were not baked but evacuated for about 1 h. [c] NaCl substrates were not baked, and water vapors were admitted into the flow-tube reactor. [d] This value should be considered as a lower limit. See text for details.

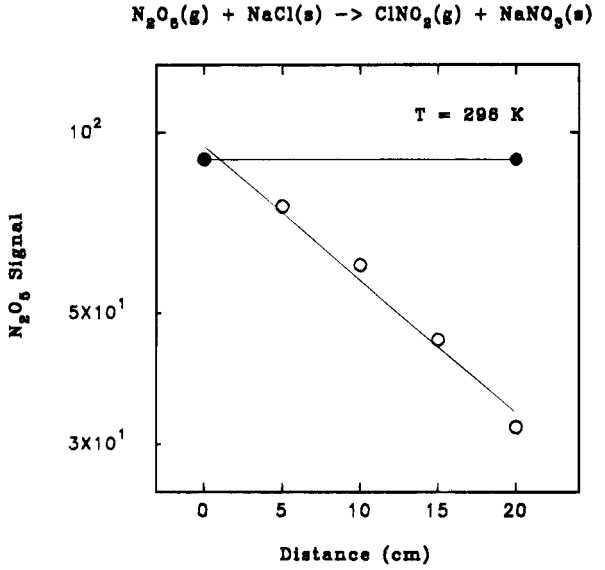

Figure 9. Loss of N_2O_5 as a function of injector position. Solid circles are for a blank experiment with no NaCl present. Open circles are for data in the presence of NaCl.

apparently very different. These γ values were based on the geometric area of the sample holder and were not corrected for the internal surface areas of the substrates. The solid NaCl samples were prepared by grinding crystalline salt into a powder, and typical grain sizes varied between 5 and 100 μm, as determined by scanning electron microscopy. If we assume the average grain size is 20 μm and use our layer model,[35,36] the corrected γ value becomes $\gamma(1) \sim 0.003$, significantly smaller than our present result at room temperature. It is possible that

TABLE 2: Summary of the Reaction Probability Measurements for the N_2O_5 + NaCl → $ClNO_2$ + $NaNO_3$ Reaction

NaCl substrates	$T = 296$ K	no. of experiments	$T = 223$ K	no. of experiments
baked[a]	$<1.0 \times 10^{-4}$	4	$<1.0 \times 10^{-4}$	3
unbaked[b]	$\approx 4.5 \times 10^{-4}$	4	$\approx 2.4 \times 10^{-4}$	6

[a] NaCl substrates were baked overnight in vacuum. [b] NaCl substrates were not baked but evacuated for about 1 h. The enhancement of the reaction probability is due to the $N_2O_5 + H_2O \rightarrow 2HNO_3$ reaction on the surfaces of the NaCl granules.

the partial HNO_3 pressures used in their experiments are greater than those used in ours, resulting in surface deactivation and, hence, a smaller observed γ value.

In a study of reaction 2, Livingston and Finlayson-Pitts used an infrared spectrometer to monitor both the reactant (N_2O_5) and the product ($ClNO_2$); a lower limit of 2.5×10^{-3} at 298 K was estimated.[16] The N_2O_5 concentration used was very large, about 1×10^{14} molecules/cm^3 (or 3×10^{-3} Torr), which is several orders of magnitude greater than atmospheric conditions. The observed γ value is significantly greater than the results listed in Table 2. The discrepancy is probably due to the estimation of the residence time, ~0.16 s, for N_2O_5 over the NaCl. In their study gaseous N_2O_5 in 1 atm of air was expanded from a 5 L bulb through NaCl packed in a cylindrical cell of cross-sectional area 3.1 cm^2 and 20 cm length into a long-pathlength infrared cell. The average flow rate was calculated from the pressure decrease in the 5 L bulb. It is rather unlikely that the gas mixture flowed through the NaCl column within such a short time unless a fast switching valve was used. Of course, this suggestion is very speculative, and further work on reaction 2 may be necessary.

TABLE 3: Reaction Probabilities for Heterogeneous Reactions Involving NaCl: Comparison with Previous Measurements

reaction	reaction probability	T, K	substrate condition	ref
HNO_3 + NaCl	1.3×10^{-2}	296	dry or slightly wet powders	this work
	$>8.0 \times 10^{-3}$	223	dry or slightly wet powders	this work
	4.0×10^{-4}	298	dry single crystals	Laux et al.[14]
	2.8×10^{-2} [a]	298	dry powders	Fenter et al.[15]
N_2O_5 + NaCl	$<1.0 \times 10^{-4}$	296	dry powders	this work
	$<1.0 \times 10^{-4}$	223	dry powders	this work
	$\approx 4.5 \times 10^{-4}$	296	slightly wet powders	this work
	$\approx 2.4 \times 10^{-4}$	223	slightly wet powders	this work
	$>2.5 \times 10^{-3}$	298	dry powders	Livingston and Finlayson-Pitts[16]
	0.03	298	wet salt aerosols	Zetzsch and Behnke[18]
	0.014−0.039	263−278	droplets	George et al.[20]
	$<2.0 \times 10^{-3}$	298	wet salt solutions	Msibi et al.[21]
$ClONO_2$ + NaCl	4.6×10^{-3}	296	dry or slightly wet powders	Timonen et al.[22]
	6.7×10^{-3}	225	dry or slightly wet powders	Timonen et al.[22]
NO_2 + NaCl	6×10^{-5} to 5×10^{-8}	298	dry powders	Vogt and Finlayson-Pitts[23]

[a] The γ value, corrected for internal surface areas, is about 0.003.

Using an aerosol smog chamber, Zetzsch and his coworkers[17−19] determined a sticking coefficient of 0.03(+0.02, −0.01) for reaction 2 at various relative humidities between 71 and 92%. This value is similar to that reported for pure water droplets.[38] In addition, this value was obtained by using an indirect complex analysis of a kinetic system containing NO_2, O_3, N_2O_5, NaCl, and H_2O in a Teflon bag. Furthermore, several previous smog chamber studies[39−41] have suggested that the reaction of N_2O_5 with H_2O forming HNO_3 occurs readily under similar conditions. In a separate study they also performed some experiments on the branching ratio of the reaction $N_2O_5 + H_2O \rightarrow 2HNO_3$ and reaction 2 using a wetted-wall column apparatus. A very high pressure of N_2O_5 about 1 Torr and similar relative humidities were used. Both reaction products, HNO_3 and $ClNO_2$, were monitored by using an infrared spectrometer coupled to a single path cell. The ratio of product yield was obtained to be $[ClNO_2]/2[HNO_3] = 2.5$. It appears that the use of very high N_2O_5 concentrations, about 6 orders of magnitude greater than that used in the present study, may be favorable to form $ClNO_2$. Because the study performed by Zetzsch and his coworkers[17−19] is very preliminary and detailed information is not available, the suggestion remains speculative.

In a very recent study, George et al.[20] studied the uptake of N_2O_5 by NaCl solutions from 262 to 278 K using a droplet train technique. The experimental conditions used are similar to those in the troposphere. They monitored the formation of nitrate in the liquid phase by ion chromatography, and therefore the detection scheme is not selective for possible reaction products, $ClNO_2$ and HNO_3. A value of $\gamma(2)$ from 0.014 to 0.039, much larger than our data of reaction 2 for dry salt, was reported. Because of the interference from the $N_2O_5 + H_2O$ reaction, their data is very close to the results reported for the uptake of N_2O_5 by water droplets[41] and also our measurement for reaction 1 (see Table 1).

Using a deposition profile in a laminar flow tube, in which the walls were coated with the NaCl substrates, Msibi et al.[21] obtained a value of 0.015 for 5% solution and <0.002 for dry salts at 45−96% relative humidity. Ion chromatography was used to monitor the NO_3^- concentrations. The production of gas phase nitric acid on the surface followed by its absorption distorted the deposition profiles; hence, a correction for this effect was required. Nonetheless, the results suggest the hydrolysis of N_2O_5 can be important, consistent with our findings discussed in the previous section.

Implications for the Lower Stratosphere and Marine Troposphere. The implications of the heterogeneous reactions studied in this paper for the stratosphere are investigated using the Caltech/JPL one-dimensional photochemical model. We shall focus on an explanation of the observed increase of HCl in the lower stratosphere after the El Chichon volcanic eruption in 1982.[3] The details of the model are described by Michelangeli et al.[4] The concentration of NaCl-containing aerosols is based on the observations of Woods et al.[2] and estimated by Michelangeli et al.[5] The frequency of a reactive collision between a gas-phase molecule and NaCl is $J_{NaCl} = {}^1/_4\gamma\bar{\omega}AN_0$, where γ is the reaction probability, $\bar{\omega}$ is the average speed of the impacting molecule ($(8kT/\pi m)^{1/2}$), A is the surface area per particle, and N_0 is the number density of particles. Using the data given by Michelangeli et al.,[5] we obtain a value of $J_{NaCl} = 1.14 \times 10^{-2}\gamma$ (s^{-1}) at 28 km. Since HNO_3 is the most abundant odd nitrogen species in the stratosphere, we shall first investigate the reaction between NaCl and HNO_3. If we adopt a value of $\gamma(1) = 8.0 \times 10^{-3}$ (from Table 1) for reaction 1, then we have $J_{NaCl} = 9.1 \times 10^{-5}$ s^{-1}. This implies that the time constant for the release of HCl from NaCl is on the order of hours. However, we believe that this sustained rate of release is unlikely because HNO_3 adsorbs on the surface of NaCl (see Figure 6a and b) and subsequent reaction may be limited by the rate of diffusion of HNO_3 through the solid aerosol. The product of the reaction between NaCl and HNO_3 is $NaNO_3$. It is unlikely that the latter will be released to the atmosphere. The accumulation of $NaNO_3$ on the aerosol surface reduces the efficiency of subsequent reactions between NaCl and HNO_3, as shown in Figure 6. Thus, we cannot adopt the straightforward value of $\gamma(1)$ from Table 1.

In modeling the time evolution of the release of HCl from reaction 1, we adopt a two-stage process, using a time-dependent γ value. In the first stage we allow the reaction to proceed with $\gamma = \gamma_0 e^{-t/\tau}$, where γ_0 is 0.008, t is the time, and τ is 30 min. The choice of 30 min is based on the following consideration. By this time we estimate that a fraction ($\sim$1/e) of the surface is covered by $NaNO_3$. With this parametrization of γ, its value would become small after about 100 min. In the second stage of our scheme we assume that the heterogeneous rate coefficient is slower by a factor of 100 due to saturation of surface sites (the choice of this factor is based on our laboratory data shown in Figure 6, and we shall discuss the sensitivity of our model results to this choice). The model is allowed to run for 6 days. The initial profile of HCl and those after 6 h and 6 days are presented in Figure 10A. The initial HCl profile is taken from the "standard" model of the stratosphere in 1982 with Cly = 1.6 ppb. The corresponding column density is 1.28×10^{15} cm^{-2}. The column density of the profile after 6 h is 8% higher than the initial column density (see Figure 10B). At the end of 6 days the column density of HCl has increased to 1.88×10^{15} cm^{-2} or about 40% greater

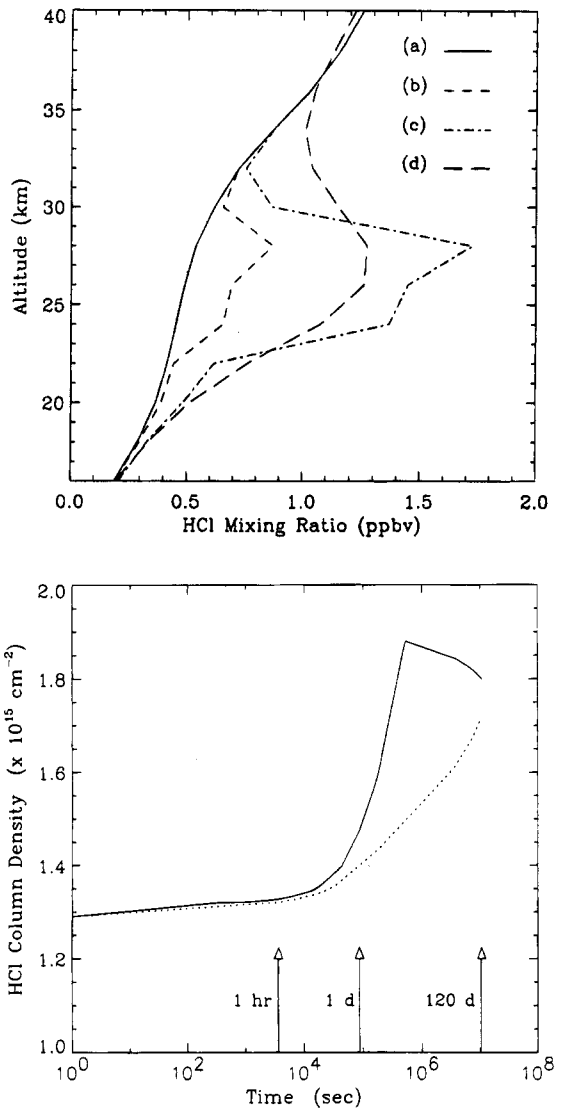

Figure 10. (A, top) Time-dependent profile showing the evolution of HCl as computed by the Caltech/JPL one-dimensional photochemical model. The standard profile (a) is given for time = 0. Profiles (b), (c), and (d) refer to times of 6 h, 6 days, and 120 days, respectively. (B, bottom) Time-dependent column density of HCl as computed by the Caltech/JPL one-dimensional photochemical model. The solid curve is the result using $\gamma_0 = 0.008$, and the broken curve is for that using $\gamma_0 = 0.0008$. See text for further details.

than the initial value. This is in good agreement with the observations.[3] Note that the bulk of the increase is in the layer of enhanced aerosol concentrations.[3,4] After this time the heterogeneous reaction is switched off (presumably due to the exhaustion of available NaCl), as further heterogeneous release of HCl will violate the observations of Mankin and Coffey.[3] The model is allowed to run for another 120 days. The main effect in this period is a gradual smoothing of the HCl profile due to eddy diffusion. Beyond 120 days the dispersion of the volcano-enhanced HCl in the atmosphere will be mostly due to the effects of horizontal motion and the one-dimensional model is no longer realistic. The time history of the HCl column density is given in Figure 10B.

Since there is considerable uncertainty in the choice of γ_0 in the model, we ran another model in which γ_0 was taken to be 0.0008, followed by a characteristic decay as in the previous case. The choice of this γ_0 value was based on the observation of a much smaller yield of HCl, about 10% of HNO_3 loss, shown in Figure 6a. The result for the column abundance of HCl is given by the broken curve in Figure 10B. It is clear that in this case the rise of HCl is much slower but is still of the right magnitude to account for the observations.[2] Values of γ_0 significantly below the above choice would not be able to explain the observations.

The modeling results on the release of HCl from reaction 1 shown in Figure 10A and B obviously depend on the choice of two arbitrary parameters. The first is the choice of the time constant $\tau = 30$ min for the initial phase of reaction that coats the surface of the aerosol with HNO_3 and $NaNO_3$. Since this time is so short compared with other atmospheric time constants, we may regard this phase as "instantaneous". During the second phase of the interaction between NaCl and HNO_3, we reduce its efficiency from the measured value by a factor of 0.01. The exact value of this reduction factor will affect the time constant for the reaction between NaCl and HNO_3 to reach saturation. For instance, if this factor were more than 0.01, release of HCl would terminate in less than 6 days. If this factor were 0.001, then the release of HCl would take 60 days. All these cases would still be consistent with the available observations. The El Chichon volcano erupted in March and April of 1982. The first observations that documented an increase of stratospheric HCl were taken in July 1982.[3] This is more than 60 days after the eruption. It is clear that to narrow down the range of uncertainty in the release rate of HCl from NaCl further laboratory experiments as well as timely volcanic observations must be carried out.

There are three other reactions that are capable of releasing HCl from NaCl in the stratosphere, involving N_2O_5, $ClONO_2$, and NO_2 (reactions 2−4). However, the concentrations of the latter species in the lower stratosphere are much smaller than that of HNO_3, and the γ values for reactions 2−4 are smaller than that for reaction 1. Hence, they will not be able to competitively react with NaCl, especially after all the surface sites are occupied by HNO or $NaNO_3$. Even if these reactions are competitive, they will just add to the production of HCl, although the time constant for the appearance of HCl would be different. The main difference between reaction 1 and reactions 2−4 is that the fomer releases HCl directly, whereas the latter release chlorine in labile forms, such as $ClNO_2$, Cl_2, or NOCl. The most likely fate of these molecules is removal by photodissociation, releasing Cl atoms. The conversion of Cl to HCl proceeds by the reaction

$$Cl + CH_4 \rightarrow HCl + CH_3 \qquad (14)$$

This reaction by itself will remove Cl in the lower stratosphere with a time constant on the order of 100 s. However, the bulk of Cl atoms will preferentially react with O_3 rather than with CH_4. Taking this into account implies that the conversion of active chlorine to HCl takes about 10 days in the lower stratosphere. Thus, the overall result of reactions 2−4 is same as that for reaction 1, with the time constant being the only difference.

In summary, we conclude that the measured reaction probability between NaCl and HNO_3 reported in this work provides an adequate explanation of the observed increase of HCl after the El Chichon eruption.

The implications of the heterogeneous reactions studied in this paper for tropospheric chemistry will now be briefly discussed. HCl has been detected in the marine troposphere with concentrations on the order of 100−1000 pptv (pptv is defined as parts per trillion in volume; see ref 42 and references cited therein). By comparison, the gas-phase chemistry predicts only about 10 pptv, consistent with the HCl profile shown in Figure 10 when extrapolated to the troposphere. Reaction 1 has been postulated to release HCl from NaCl. The most

compelling evidence in support of this mechanism is the recent measurement of HCl by Eldering et al.[12] in coastal southern California. The concentrations of HCl ranged from 39 to 1250 pptv and appeared to correlate with similar concentrations of HNO_3. We may roughly estimate the time constant for the interaction between NaCl and HNO_3 as follows. The aforementioned experiment reported concentrations of 6.3 $\mu g/m^3$ of NaCl. Assuming an average radius of 1 μm, we estimate a collision frequency of $J_{NaCl} = 1 \times 10^{-5}$ s^{-1}, where a value of γ of 1.3×10^{-2} has been taken from Table 1. At this rate, the conversion of NaCl to HCl occurs in 1 day and is fast enough to account for the observed HCl concentrations. Reactions 2 and 3 can contribute to the production of HCl but will be less important due to the lower concentrations of N_2O_5 and $ClONO_2$ and smaller γ values (see Table 1).

Acknowledgment. The research described in this article was performed at the Jet Propulsion Laboratory, California Institute of Technology, under a contract with the National Aeronautics and Space Administration. Y.L.Y. acknowledges support of NASA Grant NAGW 2204 to the California Institute of Technology. The authors are grateful to Veronica Bierbaum and Carleton Howard for helpful discussion on the development of CI mass spectrometry, Renyi Zhang for the design of the data acquisition system, and Greg Huey and Michel Rossi for sending preprints.

Note Added in Proof. In an article recently submitted to *The Journal of Physical Chemistry*, Fenter, Caloz, and Rossi reported $\gamma(1) = 0.02$ and $\gamma(2) = 5 \times 10^{-4}$ at 298 K for dry NaCl powders using a Knudsen cell reactor coupled to an electron-impact ionization quadrupole mass spectrometer. These values are consistent with our data reported in this work (see Table 3).

References and Notes

(1) Solomon, S. *Nature* **1990**, *347*, 347.
(2) Woods, D. C.; Chuan, R. L.; Rose, W. I. *Science* **1985**, *230*, 170.
(3) Mankin, W. G.; Coffey, M. T. *Science* **1984**, *226*, 170.
(4) Michelangeli, D. V.; Allen, M.; Yung, Y. L. *J. Geophys. Res.* **1989**, *94*, 18429.
(5) Michelangeli, D. V.; Allen, M.; Yung, Y. L. *Geophys. Res. Lett.* **1991**, *18*, 673.
(6) Finlayson-Pitts, B. J. *Nature* **1983**, *306*, 676.
(7) Finlayson-Pitts, B. J.; Ezell, M. J.; Pitts, J. N., Jr. *Nature* **1989**, *337*, 241.
(8) Keene, W. C.; Pszenny, A. A. P.; Jacob, D. J.; Duce, R. A.; Galloway, J. N.; Schultz-Tokos, J. J.; Sievering, H.; Boatman, J. F. *Global Biogeochem. Cycles* **1990**, *4*, 407.
(9) Pszenny, A. A. P.; Keene, W. C.; Jacob, D. J.; Fan, S.; Maben, J. R.; Zetwo, M. P.; Springer-Young, M.; Galloway, J. N. *Geophys. Res. Lett.* **1993**, *20*, 699.
(10) Cadle, S. H.; Countless, R. J.; Kelly, N. A. *Atmos. Environ.* **1980**, *16*, 2501.
(11) Solomon, P. A.; Salmon, L. G.; Fall, T.; Cass, G. R. *Environ. Sci. Technol.* **1992**, *26*, 1594.
(12) Eldering, A.; Solomon, P. A.; Salmon, L. G.; Fall, T.; Cass, G. R. *Atmos. Environ.* **1991**, *25*, 2091.
(13) Galasyn, J. F.; Tschudy, K. L.; Hubert, B. J. *J. Geophys. Res.* **1987**, *92*, 3105.
(14) Laux, J. M.; Hemminger, J. C.; Finlayson-Pitts, B. J. *Geophys. Res. Lett.* **1994**, *21*, 1623.
(15) Fenter, F. F.; Caloz, F.; Rossi, M. J. *J. Phys. Chem.* **1994**, *98*, 9801.
(16) Livingston, F. E.; Finlayson-Pitts, B. J. *Geophys. Res. Lett.* **1991**, *18*, 17.
(17) Behnke, W.; Kruger, H.-U.; Scheer, V.; Zetzsch, C. *J. Aerosol Sci.* **1991**, *22*, S609; **1992**, *23*, S933.
(18) Behnke, W.; Scheer, V.; Zetzsch, C. *J. Aerosol Sci.* **1993**, *24*, S115.
(19) Zetzsch, C.; Behnke, W. *Ber. Bunsen-Ges. Phys. Chem.* **1992**, *96*, 488.
(20) George, Ch.; Ponche, J. L.; Mirabel, Ph.; Behnke, W.; Scheer, V.; Zetzsch, C. *J. Phys. Chem.* **1994**, *98*, 8780.
(21) Msibi, I. M.; Li, Y.; Shi, J. P.; Harrison, R. M. *J. Atmos. Chem.* **1994**, *18*, 291.
(22) Timonen, R. S.; Chu, L. T.; Leu, M.-T.; Keyser, L. F. *J. Phys. Chem.* **1994**, *98*, 9509.
(23) Vogt, R.; Finlayson-Pitts, B. J. *J. Phys. Chem.* **1994**, *98*, 3747.
(24) Chu, L. T.; Leu, M.-T.; Keyser, L. F. *J. Phys. Chem.* **1993**, *97*, 7779.
(25) Chu, L. T.; Leu, M.-T.; Keyser, L. F. *J. Phys. Chem.* **1993**, *97*, 12798.
(26) Gleason, J. F.; Sinha, A.; Howard, C. J. *J. Phys. Chem.* **1987**, *91*, 719.
(27) Huey, L. G.; Hanson, D. R.; Howard, C. J. *J. Phys. Chem.* **1995**, *99*, 5001.
(28) Davidson, J. A.; Viggiano, A. A.; Howard, C. J.; Dotan, I.; Fehsenfeld, F. C.; Albritton, D. L.; Ferguson, E. E. *J. Chem. Phys.* **1978**, *68*, 2085.
(29) Fehsenfeld, F. C.; Howard, C. J.; Schmeltekopf, A. L. *J. Chem. Phys.* **1975**, *63*, 2835.
(30) Gregg, S. J.; Sing, K. S. W. *Adsorption, Surface Area and Porosity*; Academy Press: New York, 1982.
(31) Weast, R. C. *Handbook of Chemistry and Physics*, 65th ed.; CRC Press: Boca Raton, FL, 1984.
(32) Walker, R. E. *Phys. Fluids* **1961**, *4*, 1211.
(33) Kaufman, F. *Prog. React. Kinet.* **1961**, *1*, 1.
(34) Marrero, T. R.; Mason, E. A. *J. Phys. Chem. Ref. Data* **1972**, *1*, 3.
(35) Keyser, L. F.; Moore, S. B.; Leu, M.-T. *J. Phys. Chem.* **1991**, *95*, 5496.
(36) Keyser, L. F.; Leu, M.-T.; Moore, S. B. *J. Phys. Chem.* **1993**, *97*, 2800.
(37) Satterfield, C. N. *Heterogeneous Catalysis in Industrial Practice*, 2nd ed.; McGraw-Hill, Inc.: New York, 1991.
(38) Van Doren, J. M.; Watson, L. R.; Davidovits, P.; Worsnop, D. R.; Zahniser, M. S.; Kolb, C. E. *J. Phys. Chem.* **1990**, *94*, 3265.
(39) Morris, E. D.; Niki, H. *J. Phys. Chem.* **1973**, *77*, 1929.
(40) Tuazon, E. C.; Atkinson, R.; Plum, C. N.; Winer, A. M.; Pitts, J. N., Jr. *Geophys. Res. Lett.* **1983**, *10*, 953.
(41) Hatakeyama, S.; Leu, M.-T. *J. Phys. Chem.* **1989**, *93*, 5784.
(42) Singh, H. B.; Kasting, J. F. *J. Atmos. Chem.* **1988**, *7*, 261.

JP9503831